Particle Accelerators
1975, Vol. 6, pp. 245–250

NUMERICAL STUDIES OF ION-LOADED ELECTRON RINGS

J. W. POUKEY and J. R. FREEMAN

Sandia Laboratories, Albuquerque, New Mexico 87115, USA

and

M. REISER

University of Maryland, College Park, Maryland 20742, USA

(*Received December 5, 1974; in final form March 14, 1975*)

A $2\frac{1}{2}$-dimensional particle simulation code is used to study a ring of relativistic (3.5-MeV) electrons which is circulating in an applied uniform magnetic field. The ring is seeded with a small percentage of positive ions. Axial symmetry is assumed, and the transverse focusing conditions are investigated as a function of ring geometry, fraction of ions, and conducting boundaries. The mean radii of the electron and ion subrings are oscillating and electron loss occurs under some conditions. We discuss two methods which are effective in combating this loss: the inclusion of an inner conductor, and the elimination of magnetic images.

I PROBLEM

Several laboratories are attempting to use circulating rings of electrons to trap and accelerate ions to high energies.[1–5] Among the theoretical problems associated with these experiments are the oscillations and electron loss from a ring seeded with ions.

Ivanov *et al.*,[6] Laslett,[7] and Reiser[8] used a linear analysis to calculate the small-amplitude "betatron" oscillation frequencies about an equilibrium orbit in such a system. Davidson, Lawson and Mahajan[9] studied the equilibrium properties of such rings within the framework of the steady-state Vlasov–Maxwell equations. The problem of resonances due to coupling between the transverse oscillations in the electron and ion subrings was first treated by Koshkarev and Zenkevich.[10] Boris and Lee[11] performed some preliminary computer simulations of ion-loaded rings in a uniform applied magnetic field; they found that due to radial separation of the electron and ion subrings, as well as an apparent lack of axial focusing, beam blowup and particle loss occurred.

In the present paper we discuss the results of our own simulations of this problem, and we reach the following conclusions. (1) Although we confirm the results of Boris and Lee for the conditions studied by them, through the addition of an inner radial conducting boundary the electron loss may be reduced, or even stopped entirely, and in typical cases a substantial electron core will be retained. (2) By designing the radial boundaries to eliminate magnetic image forces ("squirrel cage" windings),[12] the electron loss may be reduced even further.

A schematic of the initial conditions for the problem is shown in Figure 1. We use cylindrical coordinates r, θ, z and assume θ-symmetry; thus our independent variables are r, z and time t. We use periodic boundary conditions in the z direction; thus in Figure 1 there are also rings at

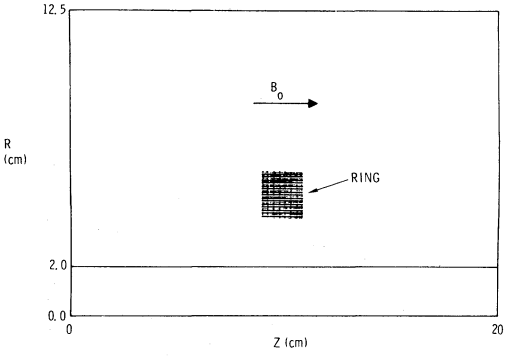

FIGURE 1 Schematic of initial conditions for the problem. Boundaries at $r = 2$ and 12.5 cm are conductors; periodic boundary conditions are used in z. Azimuthal symmetry about the z-axis is assumed.

$z = -10$ and $+30$ cm. The z-separation of 20 cm between rings is much larger than the (average initial) ring radius of 5 cm, so that we are in effect solving the problem of a ring by itself between infinitely long radial boundaries. To check that this is so, several of our solutions were also obtained with a ring separation of 40 cm, and no significant differences were observed.

The assumption of axial symmetry in our system implies that any effects that result from, or lead to, variations in charge and current distribution with azimuth angle θ are excluded in the computer simulation. Examples of effects which we do *not* treat are coherent off-centering of one or both particle subrings, electron-ion coupling resonances, and the negative mass instability. Our main objective is a self-consistent study of the equilibrium problem; in particular, the effects of beam dimensions, positive ions and conducting boundaries.

The parameter values in this paper were chosen to be relevant to the Maryland electron ring experiments.[4,5] Thus in Figure 1 the inner and outer radial conducting boundaries (both at zero potential) are at $a = 2$ cm and $b = 12.5$ cm. The average initial ring radius of $R = 5$ cm was chosen so that $R^2 = ab$, which is the condition that the radial position of a thin-shell electron beam be chosen to minimize the potential.[13,14]

The only applied field is an axial magnetic field $B_0 = 0.266$ T, chosen for equilibrium of a $\gamma = 7.85$ beam (thus the initial kinetic energy, all θ-directed, of the beam electrons is 3.5 MeV). The beam self-fields are obtained from the equations

$$\frac{\partial^2 A_\theta}{\partial z^2} + \frac{\partial}{\partial r}\left(\frac{1}{r}\frac{\partial}{\partial r}(rA_\theta)\right) = -\mu_0 j_\theta \tag{1}$$

$$\frac{\partial^2 \phi}{\partial z^2} + \frac{1}{r}\frac{\partial}{\partial r}\left(r\frac{\partial \phi}{\partial r}\right) = -\frac{\rho}{\varepsilon_0} \tag{2}$$

$$E_\theta = -\frac{\partial A_\theta}{\partial t} \quad E_r = -\frac{\partial \phi}{\partial r} \quad E_z = -\frac{\partial \phi}{\partial z} \tag{3}$$

$$B_\theta = \frac{\mu_0}{r}\int_0^r j_z\, r\mathrm{d}r \quad B_r = -\frac{\partial A_\theta}{\partial z} \quad B_z = \frac{1}{r}\frac{\partial}{\partial r}(rA_\theta) \tag{4}$$

where A_θ is vector potential (θ-component), (j_r, j_θ, j_z) is electron current density, ϕ is electric potential, and (E_r, E_θ, E_z) and (B_r, B_θ, B_z) are the electric and magnetic self-fields, caused by space charge and induction. Note that radiation fields and induction fields due to $\partial B_\theta/\partial t$ have been neglected, which can be justified by estimating their magnitudes.

The charge density $\rho = e(n_i - n_e)$, where n_i is ion density and n_e is beam (electron) density. In Figure 1 the ions are assumed to be already present in the ring; we define f as the initial number N_i of ions, divided by the initial number N_e of electrons in the ring:

$$f = N_i/N_e. \tag{5}$$

The equation of motion for the electrons is

$$\frac{\mathrm{d}\mathbf{V}}{\mathrm{d}t} = -\frac{e}{m\gamma}\left(\mathbf{E} - \frac{\mathbf{V}\cdot\mathbf{E}}{c^2}\mathbf{V} + \mathbf{V}\times\mathbf{B}\right) \tag{6}$$

where m, e are electron rest-mass and charge, c is the speed of light, $\gamma = (1 - V^2/c^2)^{-1/2}$, and $\mathbf{V} = (V_r, V_\theta, V_z)$ is the electron velocity. For the nonrelativistic ions we have

$$\frac{\mathrm{d}\mathbf{V}_i}{\mathrm{d}t} = \frac{e}{m_i}\mathbf{E} \tag{7}$$

where m_i, $\mathbf{V}_i$ are ion mass and velocity, and we neglect magnetic forces and θ-motion of the ions. This is justified since the dominant effects in regard to the focusing problem are the radial Coulomb forces between electrons and ions.

II CODE

The simulation particles, each of which represents a ring of real particles, are initialized by distributing them (both electrons and ions) uniformly over the cross section indicated in Figure 1. The electrons are given initial velocity $V_\theta = 2.97556 \times 10^8$ m/sec, the ions start at rest. The basic cycle in the code is then to solve in turn for (1) densities, (2) potentials and fields, and (3) new particle velocities and positions. The densities are found by standard area weighting techniques.[15–17] The solvers for Eqs. (1) and (2) are based on the fast Fourier transform method of Hockney.[18] The "particle pusher" step in the cycle is similar to that used recently in solving diode problems[19]; given the fields at time step n, the particles are advanced to step $n + 1$ via a predictor-corrector method.

Our typical r-z mesh is 33×33, time step 5×10^{-12} sec (cyclotron period is about 10^{-9} sec), number of simulation electrons and ions 2000 and 400, respectively. That these choices are adequate for the problem at hand was checked by trial-and-error variation. Our scheme is second-order accurate in the time and space steps, except for E_θ in Eq. (3), which is first-order. Fortunately,

we find E_θ to be relatively small (but not negligible).

Since it is costly to use the full m_i/m value, we have generally used artificially light ions, with $m_i/m = 100$. As a check, one case was repeated with $m_i/m = 400$. Thus in the results presented below, the ion behavior occurs on a time scale at least 4 times faster than in reality, and in giving times for electron loss, etc., our computed results will always err on the pessimistic side.

The boundary conditions used are periodic in z, and perfectly conducting at $r = a$ and $r = b$ ($\phi = A_\theta = 0$, where A_θ does not include the applied B_0). The exception is the several cases to be discussed below in which it was desired to have the radial boundaries be electrically, but not magnetically, conducting. In these cases the $\phi = 0$ condition was still used, but the A_θ boundary values were determined self-consistently (every few hundred time steps is sufficient) by integrating over the internal current loops.

III THEORETICAL CONSIDERATIONS

Before presenting the results of our numerical simulation studies, let us briefly examine the problem of an ion-loaded ring from the point of view of the linear analyses mentioned above. The betatron oscillation frequencies, ν_r and ν_z (normalized to $eB_0/m\gamma$), of the electrons about the equilibrium orbit are a measure for the radial and axial force balance in the toroidal beam; in fact, ν_r^2 and ν_z^2 are directly proportional to the focusing forces in each direction. If the effects of self-fields are neglected, the radial and axial betatron frequencies in a uniform magnetic field are $\nu_r = 1$ and $\nu_z = 0$, respectively. Thus, the major problem is the absence of focusing forces in axial direction. If self-fields are included, one obtains the following formula[8]:

$$\nu_z^2 = -\frac{4\mu R^2}{\delta_b(\delta_a + \delta_b)\beta^2}\left(\frac{1}{\gamma^2} - f\right) - \frac{\mu P}{2}. \quad (8)$$

R is the major radius of the ring, $2\delta_a$ and $2\delta_b$ are the minor dimensions in the radial and axial directions. The parameters μ and P are defined as

$$\mu = 4.58 \times 10^{-14}\frac{N_e}{R\gamma}, \quad (9)$$

where R is measured in cm, and

$$P = 2\ln\frac{16R}{\delta_a + \delta_b}. \quad (10)$$

The first term in Eq. (8) represents the "linear-beam" effect, i.e., the balance between Coulomb repulsion and magnetic attraction present in a straight beam of relativistic electrons with stationary positive ions. It is defocusing as long as $f < 1/\gamma^2$. The second term in Eq. (8) represents the "toroidal" effect, i.e., the forces acting on an electron due to the toroidal shape of the beam. This term is always defocusing. Thus, in order to obtain a net focusing force in the axial direction ($\nu_z^2 > 0$), the fraction f of stationary positive ions must exceed the Budker limit[20] ($f = 1/\gamma^2$) by an amount large enough to compensate for the toroidal defocusing effect.

If conducting boundaries are present, the image fields due to induced charges and currents produce additional terms in the equations for ν_r^2 and ν_z^2 which were discussed by Laslett.[7] With regard to ν_z^2, the electric image forces due to coaxial conducting boundaries outside and/or inside of the ion-loaded ring are focusing while the magnetic image forces have a defocusing effect. The magnetic image forces can be suppressed by preventing azimuthal current flow in the conducting boundary. This is accomplished by use of long, thin metallic rods or strips in a squirrel-cage-type arrangement.[12] The "squirrel-cage" effect alleviates the focusing problem and allows the use of a smaller number of positive ions which is desirable for more efficient acceleration by the expansion method employed in electron ring accelerator experiments. Detailed studies of the "squirrel-cage" focusing method were made by Hofmann,[21] and the effect was confirmed in recent experiments at Garching.[2]

The linear analysis on which the previous discussion of focusing forces is based is possible only for thin rings in which the minor dimensions are small compared to the major radius. In addition, the assumptions inherent in such a theory provide only a rough approximation to the behavior of the actual system. In actual experiments, the situation may differ significantly from these models. At the University of Maryland, for instance, the electron ring is being formed from a long rotating sheet beam with axial dimensions initially much larger than the radial width. These facts motivated the numerical simulation studies reported in this paper. Apart from the important problem of axial focusing in beams with different cross sections, we were also interested in the radial motion. In particular, we wanted to see if the use of an inner conductor would reduce the radial separation of electron and ion subrings found in

the simulation studies by Boris and Lee mentioned earlier.[11]

IV NUMERICAL RESULTS

We begin the discussion of our computer results with the case shown in Figure 1. The initial ring cross section was assumed to be rectangular with $\Delta r_b = 2\delta_a = \Delta z_b = 2\delta_b = 2$ cm, the total number of electrons was $N_e = 10^{13}$ and the fraction of ions was $f = 0.1$. We should note that in the absence of image effects due to the boundaries these parameters would yield a value of $\nu_z \approx 0.0815$, from Eq. (8), i.e., a very weak focusing force in the axial direction.

Figure 2 shows $B_z(r)$ through the center of the ring (i.e., at $z = 10$ cm) at $t = 0$. Note that the current in the ring (value is 1.5 kA here) is only able to reduce the B_z field slightly below the vacuum value (2.66 kG).

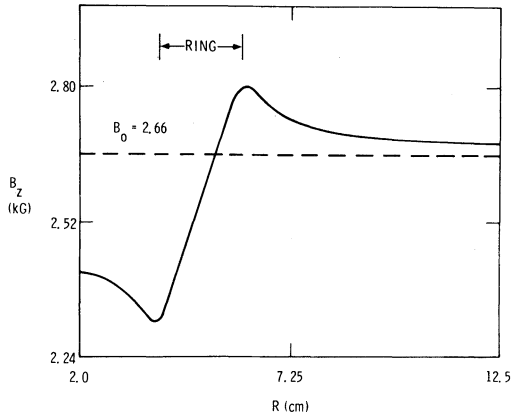

FIGURE 2 $B_z(r)$ at $z = 10$ cm, $t = 0$ for the case $f = 0.1$, $N_e = 10^{13}$, $\Delta r_b = \Delta z_b = 2$ cm, inner conductor present. The applied B_0 is 2.66 kG.

The potential well made by the electrons was found to oscillate slightly about a mean value of 1.8×10^5 V. If this value is multiplied by $2/\delta_b = 2 \times 10^2[\text{m}^{-1}]$ one gets a maximum electric field ("holding power") of 36 MV/m. The positive ions will oscillate in this potential well. The electrons, on the other hand, will oscillate or be lost from the ring depending upon the parameters. For the case under consideration, $V_\theta B_r \geq E_z$, or $v_z^2 > 0$, initially for all electrons, so the beam pinches inward in z. The periods of oscillation for a randomly selected ion and electron are $\tau_{re} = 1.03$, $\tau_{ze} = 8.1$, $\tau_{ri} = 4.36$, $\tau_{zi} = 5.9$ where the times are in nanoseconds and the subscript "re," for example, refers to "radial" and "electron." (Note that the ion times are for the mass-ratio-100 ions.) For comparison, the betatron frequency formulas of Ref. 8 [see also Eq. (8) above] give $\tau_{re} = 1.01$ and $\tau_{ze} = 13$ nsec (or $\nu_r = 1.04$, $\nu_z = 0.081$), leading to a not unreasonable comparison considering that the analytic formulas apply only to small, linear oscillations and involve several simplifying assumptions, such as stationary ions and absence of conducting boundaries.

In addition to the incoherent particle oscillations, there are coherent oscillations of the mean radii of the electron and ion subrings as a function of time.

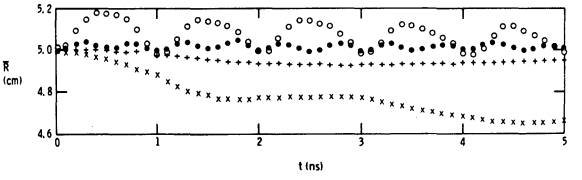

FIGURE 3 Average electron and ion radii vs. time for case $f = 0.1$, $N_e = 10^{13}$, $\Delta r_b = \Delta z_b = 2$ cm. Solid dots: electrons, with inner conductor; +: ions, with inner conductor. Open circles: electrons, no inner conductor; ×: ions, no inner conductor. Electron cyclotron period is 1.05 nsec.

Figure 3 shows the average electron and ion radii vs. time. Note that the electrons tend to remain slightly outside the ions. Also shown are the results obtained from the code by running a case which is identical in all respects to the one under discussion, except that the inner radial conductor has been removed (as in Ref. 11). In this latter case, the oscillations of the mean radii are much more pronounced, and the separation of the electron and ion subrings is considerably larger. Thus one would expect the beam to hold together better when an inner conductor is present, and this expectation is verified by Figure 4, which shows particle movie frames (electrons only) for the two cases at 7 nsec. With an inner conductor the beam is still intact, whereas without an inner conductor the beam is slowly evaporating away.

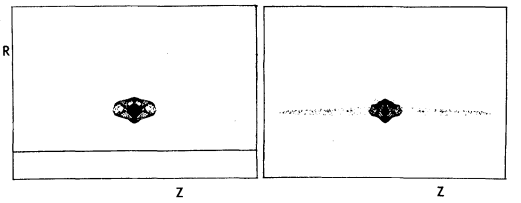

FIGURE 4 Electrons at 7 nsec for the same cases as Fig. 3. Left side: with inner conductor. Right side: no inner conductor.

Note that the beam cross sections at 7 nsec are no longer rectangular. In fact, the particle oscillations discussed above cause a constantly changing envelope of both the electron and ion subrings. To the extent that one may separate "oscillations in mean radius" from "envelope changes," loss of electrons seems to be associated more with the latter, because the radial restoring forces are stronger ($v_r^2 > v_z^2$) than the z-forces, i.e., beam loss is always in z, never in r. We note that attempts to reduce oscillations in this case by shifting the initial ring center outward to the "correct" equilibrium radius[11] (we tried $\Delta R = 0.2$ cm, with and without inner conductor) gave no substantial difference from the above results.

Next we consider the effect of shape. If we repeat the above case ($N_e = 10^{13}$, $f = 0.1$, with inner conductor, 2 × 2 cm cross section) but rotate the initial beam by 45° in the r-z plane, we obtain the solution shown in Figure 5. This shows the r-z

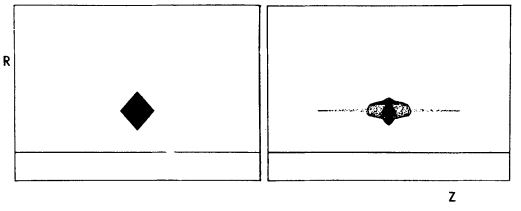

FIGURE 5 Electrons at $t = 0$ (left side) and 7 nsec (right side) for case $f = 0.1$, $N_e = 10^{13}$, inner conductor present, initial r-z cross section rotated by 45°.

cross section of the electrons at $t = 0$ and $t = 7$ nsec. The results are similar to the previous solution (compare the right side of Figure 5 with the left side of Figure 4) except for the loss of a small fringe of the beam. This suggests that the dependence on initial shape is rather weak, at least as long as this "thin-ring" geometry is used.

Next we consider beams which are initially elongated in the z-direction, which is the case in the Maryland experiment, since the ring is formed there by beam injection through a cusp magnetic field.[4,5] If we start with $\Delta r_b = 1$ cm, $\Delta z_b = 4$ cm, $f = 0.1$, $N_e = 10^{13}$, and use an inner conductor, we find that initially $V_\theta B_r > E_z$ so the beam begins by pinching in z. However, the envelope variations referred to above cause considerable beam loss after this first inward z-pinching, and at $t = 17$ nsec the situation is as shown in Figure 6. Here, the electrons are on the left and the ions are on the right. We note that although the electrons are spread over the system length, there is an apparent core at the center which

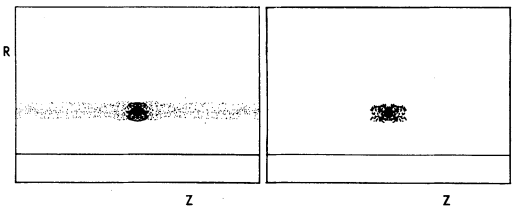

FIGURE 6 Electrons (left side) and ions (right side) at 17 nsec for case $f = 0.1$, $N_e = 10^{13}$, $\Delta r_b = 1$ cm, $\Delta z_b = 4$ cm, inner conductor present.

contains about two-thirds of the initial beam. The ions, on the other hand, are still clustered near their initial position.

If we repeat this last case but start with $f = 0.05$, we find that at $t = 0$, $E_z > V_\theta B_r$ for the beam electrons, so beam loss begins immediately. However, at late times this inequality is reversed, and an electron core persists of about 40% of the original beam. Again, the ions remain near their initial location, except for the ever-present oscillations in the potential well of the electrons. The depth of this well in this case begins at 1.6×10^5 V, and becomes gradually less deep as beam electrons are lost; the depth at 20 nsec is 1.0×10^5 V.

Recalling that our boundary conditions in z are periodic, one might ask if this core of electrons is at least partly caused by electrons which leave one end and enter the other. To check this, the $f = 0.05$ case above was done with periodic field conditions but particle-absorbing walls at the ends, and the results were as given above (specifically, at $t = 21$ nsec, 58% of the original electrons were left in the system, and 38% were in the core ($\Delta z = 2$ cm). We tentatively conclude that for at least tens of nanoseconds the ion-loaded rings tend toward a state in which the "effective f" is 10–15%.

Finally, we consider the effects of removing the magnetic images. Experimentally this is accomplished by replacing the conducting radial boundaries by squirrel-cage boundaries, in which azimuthal currents cannot flow but which remain conductors electrostatically.[12,21] The way in which this is done in the code was discussed in Section II.

For the case $\Delta r_b = 1$ cm, $\Delta z_b = 4$ cm, $f = 0.05$, inner conductor present (i.e., the case just discussed but with no magnetic image forces), we find that initially $V_\theta B_r$ is larger than when the magnetic images were included, in fact sufficiently larger to make $V_\theta B_r > E_z$ at $t = 0$. Thus we expect, and find, that the electron evaporation rate is much smaller when the images are absent. In fact, by repeating this case for other f values, we find that even a 2%

ion-loaded ring, with no images, evaporates more slowly than a 5% ion-loaded ring, with images. Specifically, Table I shows the percentage of the initial ring left in the system and in the core at 16 nsec. "Core" is defined by the central $\Delta z = 2$ cm region.

TABLE I

Percentage of initial ring electrons left in system and in core at $t = 16$ nsec.

Case	% left, system	% left, core
$f = 5\%$, with images	63	37
$f = 5\%$, no images	93	52
$f = 2\%$, no images	79	37

The electron ring at $t = 0$ and 16 nsec is shown for the $f = 2\%$, no-magnetic-image case in Figure 7. In a sense it is our best solution, even though over half the ring has been lost, since it has a small initial f, and f is still only 5% at 16 nsec, and all the ions remain trapped in the core (well depth at 16 nsec is 1.1×10^5 V). The maximum E_z in the ring (holding power) is 2.7×10^6 V/m (at 16 nsec).

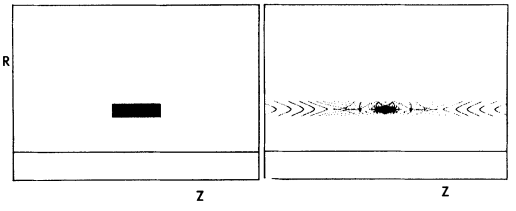

FIGURE 7 Electrons at $t = 0$ (left side) and 16 nsec (right side) for case $f = 0.02$, $N_e = 10^{13}$, $\Delta r_b = 1$ cm, $\Delta z_b = 4$ cm, inner conductor present, no magnetic image forces.

V CONCLUSION

We conclude that in an electron ring in a uniform magnetic field and loaded with a small percentage of ions, under the conditions studied here, electron losses may occur due to force imbalance, particularly in the axial direction. We have studied two ways in which these losses may be slowed, and perhaps even cured: the use of an inner conductor and the removal of magnetic images. We have demonstrated the beneficial effects of these conditions using a $2\frac{1}{2}$-dimensional particle simulation code to solve the equations of a somewhat idealized model. While the demonstration has actually only been carried out for parameters relevant to the University of Maryland static-field accelerator,[4,5] it is hoped that the conclusions are general enough to be of interest to anyone involved in the electron-ring method of ion acceleration.

ACKNOWLEDGEMENT

This work was sponsored by the U.S. Atomic Energy Commission and the National Science Foundation. The authors wish to thank Dr. Jackson Laslett for useful comments, which helped to clarify some of the basic premises and conclusions of this study.

REFERENCES

1. V. P. Sarantsev, *Proc. 8th Int. Conf. on High Energy Accelerators*, CERN 1971, p. 391.
2. C. Andelfinger, W. Dommaschk, I. Hofmann, P. Merkel, V. Schumacher, M. Ulrich, *Proc. 9th Int. Conf. on High Energy Accelerators*, SLAC, Stanford, Cal., 1974, p. 218.
3. W. W. Chupp, A. Faltens, E. C. Hartwig, D. Keefe, G. R. Lambertson, L. J. Laslett, W. Ott, J. M. Peterson, J. B. Rechen, A. Salop, and R. W. Schmieder, *Proc. 9th Int. Conf. on High Energy Accelerators*, SLAC, Stanford, Cal., 1974, p. 235.
4. M. Reiser, IEEE Trans. Nucl. Sci., **NS-20**, No. 3, 310 (1973).
5. W. W. Destler, A. Greenwald, D. W. Hudgings, H. Kim, P. K. Misra, M. P. Reiser, M. J. Rhee, and G. T. Zorn, *Proc. 9th Int. Conf. on High Energy Accelerators*, SLAC, Stanford, Cal., 1974, p. 235.
6. I. N. Ivanov, et al., JINR Report P9-4132, Dubna (1968).
7. L. J. Laslett, Technical Reports ERAN **30**, (1969) and ERAN **200**, (1972), Lawrence Radiation Laboratory, Berkeley, California.
8. M. Reiser, *Part. Accel.*, **4**, 239 (1973).
9. R. C. Davidson and J. D. Lawson, *Part. Accel.*, **4**, 1 (1972); R. C. Davidson and S. M. Mahajan, *Part. Accel.*, **4**, 53 (1972).
10. D. G. Koshkarev and P. R. Zenkevich, *Part. Accel.*, **3**, 1 (1972).
11. J. P. Boris and R. Lee, *Record of 11th Symposium on Electron, Ion, and Laser Beam Technology*, Ed. by R. F. M. Thornley, San Francisco Press, 1971, p. 535.
12. G. V. Dolbilov, et al., JINR Report P9-4737, Dubna (1969).
13. M. Reiser, IEEE Trans. Nucl. Sci., **NS-20**, No. 3, 318 (1973).
14. J. W. Poukey and J. R. Freeman, *Phys. Fluids*, **17**, 1917 (1974).
15. R. L. Morse, in *Methods in Computational Physics*, edited by B. Alder, S. Fernbach, and M. Rotenberg, (Academic, New York, 1970), **9**, p. 213.
16. C. K. Birdsall, A. Bruce Langdon, and H. Okuda, in Ref. 15, p. 241.
17. J. P. Boris, in *Proc. 4th Conf. on Numerical Simulation of Plasmas*, edited by J. P. Boris and R. A. Shanny (Office of Naval Research, Virginia, 1971), p. 3.
18. R. W. Hockney, in Ref. 15, p. 136.
19. J. W. Poukey, J. R. Freeman, and G. Yonas, *J. Vac. Sci. Technol.*, **10**, 954 (1973).
20. G. I. Budker, CERN *Symposium on High Energy Accelerators*, **1**, p. 68, 1956.
21. I. Hofmann, Report IPP 0/16, Max-Planck-Institut f. Plasmaphysik, Garching, May 1973.